SHAPING, DEGRADATION AND DRUG RELEASE OF BIOSOURCED PARTICLES MADE FROM ACRYLATED VEGETABLE OILS

Chaohe HU[1, 2], Estelle LU[1, 2], Lucie LACOUR[1, 2], Nicolas DELSUC[3], Bruno BRESSON[4], Jean-Maurice MALLET[3], Jacques FATTACCIOLI[1, 2*]

1. UMR 8640 PASTEUR, Département de Chimie, École Normale Supérieure, PSL Université, 24 rue Lhomond, 75005 Paris, France.

2. Institut Pierre-Gilles de Gennes (IPGG), 6 rue Jean Calvin 75005 Paris, France

3. UMR 7203 LBM, Département de Chimie, École Normale Supérieure, PSL Université, Sorbonne Université, CNRS, 24 rue Lhomond, 75005 Paris, France

4. UMR 7615 SIMM, École Supérieure de Physique et de Chimie Industrielles Paris, PSL University, 10 Rue Vauquelin, 75005 Paris, France

Corresponding author: jacques.fattaccioli@ens.psl.eu

KEYWORDS

Bio-sourced polymer, Vegetable oil, acrylated epoxidized soybean oil, microparticle, colloid, microfluidics

SYNOPSIS

Acrylated epoxidized soybean oil is used as a biosourced material to fabricate sophisticated, functional and degradable microparticles using microfluidics

ABSTRACT (200 words max)

The widespread employment of petroleum-based polymers is the cause of unsolved environmental problems, such as the pollution by microplastics. In this context, biodegradable plastics have attracted attention as new materials that can replace conventional ones in certain applications, especially those made from renewable resources such as acrylated epoxidized soybean oil (AESO). While AESO has been shown to be used efficiently as a plasticizer or coating material, we show here that it can be used to make microparticles of simple and sophisticated shapes, including core-shell structures, using bulk shearing or microfluidic techniques. After characterizing the polymerization conditions, we show that these particles are degradable in mild chemical or enzymatic conditions, and that they can encapsulate fluorescent probes or hydrophobic molecules of therapeutic interest. Finally, we show that they can release these molecules using a well defined mechanism in simulated digestion fluids.

INTRODUCTION

The widespread employment of petroleum-based polymers is associated with a series of environmental problems that have been a concern in recent decades, such as energy crisis and environmental pollution by microplastics. Nowadays, over 7% of oil, gas and their derivatives are produced into polymer materials[1], most of them being non-recyclable and non-degradable, which leads to serious ecological deterioration. Fortunately, abundant renewable resources such as cellulose [2], chitosan [3,4],alginate [4], lignin [5] and vegetable oils [6].

Vegetable oils and their derivatives are the most promising candidates as raw source of biobased materials since they offer numerous benefits including easy access, low cost, wide range of source, renewability and degradability [7]. Interestingly, the existence of unsaturated bonds in molecules composing vegetable oils opens up opportunities for easy modifications and functionalizations. Recently, there is a growing research interest

to develop new preparation strategies [8] and applications [9–12] of vegetable oil-based materials.

Acrylated epoxidized soybean oil (AESO) stands out as a prominent derivative of vegetable oil, resulting from the successive epoxidation and esterification of soybean oil, as outlined in studies [13]. In this process, carbon-carbon double bonds undergo opening and modification with acrylate and hydroxyl groups. The active acrylate group on the molecule enables AESO to serve as a monomer for rapid polymerization, facilitating the preparation of thermoset polymers [14,15].

The remarkable properties of AESO, including low toxicity, excellent compatibility, reliable adhesion, and swift curing, have paved the way for exciting applications. For instance, Liu et al. [16] utilized UV-cured AESO (named pAESO in the following) as a coating to enhance the hydrophobicity of natural fiber grains-flax composites, mitigating mechanical degradation caused by water swelling. Fernandes et al. [17] explored the potential of bacterial cellulose/pAESO composites as an environmentally friendly alternative to leather. Miao et al.[18] introduced a method for fabricating highly biocompatible and porous scaffolds through 3D laser printing based on AESO polymerization, highlighting its shape memory property—capable of being fixed in a temporary shape at -18 °C and fully recovering at 37 °C. Additionally, Baştürk et al. [19] demonstrated the promising application of UV-cured AESO as a substrate for loading phase change materials in thermal energy storage.

However, the majority of research on AESO-based polymers has predominantly focused on additives for composites or bulk materials, primarily due to their inherent poor mechanical properties [14]. Notably, examples on the preparation and application of polymerized AESO particles are very scarce [20]. This paper aims to fill this gap by presenting a straightforward approach to fabricate pAESO particles. In this method, an emulsion is formed by dispersing AESO containing a photo-initiator into droplets, followed by UV-induced emulsion polymerization for cross-linking. Fourier-transform infrared (FTIR) microscopy was employed for the evaluation and optimization of the polymerization process. Furthermore, we introduce a "one-pot" microfluidic device for continuous fabrication, integrating flow-focusing technology and a UV exposure zone.

This system can be customized to shape the synthesized pAESO particles as needed, which we further complexify into pAESO capsules. Additionally, we conducted characterization studies, degradability, and the ability to load fluorescent molecules, demonstrating the versatile application potential of these particles.

RESULTS

Principle and polymerization of the AESO droplets

The specific formulation protocol for preparing solid pAESO particles is outlined in **Figure 1A** and detailed in the **Supplementary Information** section. In summary, the initial step involves diluting AESO, an epoxy acrylated vegetable oil with an 85 wt.% concentration, in 1-octanol to reduce its viscosity by two orders of magnitude **Figure S2** and enhance its processability. To initiate the photopolymerization of the oil, 0.4% (w/v) of an oil-soluble, UV-sensitive photoinitiator (Irgacure 819) is added to the AESO/octanol solution.

For droplet fabrication, the above solution is mixed with an aqueous solution containing a surfactant (Pluronic F-68) at a concentration of 15 wt.% and a viscosifier (Sodium alginate) at a concentration of 2 wt.%. The mixture is then subjected to shear using a vortex mixer to produce polydisperse droplets similar to the ones shown in **Figure 1B**. Subsequent to droplet formation, the emulsion is rinsed with a PB-Tween 20 solution to eliminate the surfactant and viscosifying agent. The droplets are then exposed to UV light (UV lamp, 325-600 nm, 60 mW/cm² ± 10%) for 2 minutes to initiate photopolymerization. During this step, the photoinitiator generates primary free radicals, initiating the polymerization of the acrylate groups in the AESO molecule, resulting in particle formation [21].

As illustrated in **Figure 1C** and **Figure S1B**, the synthesized pAESO particles maintain a spherical and smooth surface, with an average diameter of 34.7 ± 10.1 µm (Coefficient of variation CV = 29.12%, see **Figure 1D**). The polymerization process of AESO

droplets is investigated through Fourier-transform infrared (FTIR) microscopy to directly observe changes in the molecular structure of AESO in the suspension before and after UV irradiation. To avoid overlap with a strong IR absorption peak (1635 cm^{-1}) [22] of water used as a solvent, deuterium oxide (D_2O) is employed as the continuous phase. The absorption peak corresponding to the scissors-bending mode of D-O-D shifts to a lower wavenumber (1200 cm^{-1}) [23] and does not overlap with the characteristic signal. **Figure 1E** shows the brightfield and the heat map images of uncrosslinked and crosslinked AESO droplets (0.4 wt.% photoinitiator, 2 min UV exposure). The heat map is computed from 1635 cm^{-1}, which corresponds to the absorption peak value of the C=C bond. It's obvious that the intensity strongly weakens after UV exposure. In order to increase the precision, we select the droplets and particles with large size as the study objects due to the low spatial resolution of the equipment (5.5 µm/pixel). **Figure 1F** shows the comparison of the FTIR spectra of single AESO droplets and particles marked with the dotted cross in the corresponding optical images. We clearly observe the decreasing of the absorption peak of acrylate moiety at 1620-1635 cm^{-1} (blue region in **Figure 1F**) for bending vibration of C=C and at 1405 cm^{-1} (green region in **Figure 1F**) for the in-plane deformation of -CH2. Additionally, the multiple absorption of carbonyl (C=O) derived from the ester group of triglycerides and acrylates transforms into a single peak (red region in **Figure 1F)**. It is attributed to the formation of the saturated ester group in the acrylates following their polymerization. All of these changes in IR absorption can clearly confirm the occurrence of the reticulation of pAESO.

Optimization of the photopolymerization advancement

As highlighted before, FTIR microscopy is well suited to analyze microparticle chemical structure and thus to optimize qualitatively the conditions of the polymerization and evaluate the influence of parameters such as photoinitiator concentration and UV exposure duration. Indeed, AESO crosslinking is a consequence of the breaking and interconnection of carbon-carbon double bond (C=C) from the acrylate group, the C sp2 carbon becoming sp3 Hence, the reaction advancement can be evaluated by monitoring the disappearance of the C=C bound during the polymerization [15,24].

Briefly, we calculate the integration ratio of the absorption of 1600-1660 cm^{-1} (C=C) to 1660-1800 cm^{-1} (C=O, used as a reference), for each pixel inside the droplet or particle, the maximum ratio is picked to represent the relative AESO conversion of this droplet or particle for comparison. For each sample, we average the measurements over N > 10 droplets or particles to improve the reliability of our measurements. We fix the UV exposure time to 2 min and vary the concentration of initiator from 0 to 2 wt.% to study the effect of concentration of initiator. **Figure S3A** shows that the conversion increases following the increase of initiator concentration, which means the large concentration can promote the polymerization. Meanwhile, in order to optimize the exposure time, 0.2 wt.% of Irgacure 819 is employed for each sample and exposition times were varied from 2 to 8 min. As shown in **Figure S3B** there is no obvious difference ($p<0.05$) for the samples exposed to different polymerization times.

Fabrication of monodisperse AESO particles using microfluidics.

Utilizing a vortex mixer offers a convenient approach for synthesizing AESO particles; however, the resulting broad size distribution poses a challenge in controlling the preparation, thus limiting their potential applications. In our efforts to enhance size uniformity and achieve continuous production of monodisperse pAESO particles, we have designed a PDMS microfluidic chip that integrates a flow focusing cross-junction (width: 40 μm) and a serpentine channel (length: 11 mm, width: 100 μm). Within this chip, droplets are generated and polymerized using a microscope objective and UV illumination, as depicted in **Figure 2A** and **Figure 2B**. In contrast to traditional PDMS chips directly bonded onto glass, our approach involves the use of a thin PDMS intermediate layer on the glass slide before binding. This method creates a homogeneous substrate surface with the same material as the channel wall, illustrated in the cross-section drawing of the channel in **Figure 2A**. Immediately following plasma bonding, we enhance the channel surface's hydrophilicity by functionalizing it with a PVP solution to prevent wetting by the oil phase during droplet generation [25]. For the microfluidic experiment, a more diluted AESO with a concentration of 65 wt.% was employed to address flow resistance and emulsification efficiency.

Figure 2C illustrates the morphology of the AESO particles prepared using the microfluidic device. As seen in **Figure 2D**, the particles exhibit a narrow size distribution with an average diameter of 46.6 ± 2.67%. The average diameter can be easily tuned by adjusting the inlet pressure ratio between the continuous and dispersed phases, as depicted in **Figure S4**. While the particles polymerized within the microfluidic chip are not readily dispersible in aqueous solvents, as shown in **Figure 2E**, they disperse perfectly in acetone. SEM observation reveals a solid core with a gel-like structure on the outer part of the particles, as illustrated in **Figure 2F**.

To render the particles dispersible in water, we collect them from the microfluidic chip and redisperse them in an acetone solution containing a photoinitiator (0.4 wt.% Irgacure 819). Subsequently, they are exposed to UV for 2 minutes. Following this step, the particles exhibit excellent dispersibility in both an aqueous buffer and acetone, as depicted in **Figure 2E**, and the gel-like outer shell of the droplets is no longer visible in the SEM pictures (see **Figure 2F -UV**).

Generation of AESO particles with complex shapes.

The microfluidic flow focusing setup described above can be modified slightly to produce biphasic droplets, ultimately resulting in the fabrication of AESO particles with intricate morphologies. The basic principle involves incorporating a second dispersed phase, namely silicon oil, which is immiscible with both water and AESO. The biphasic droplets are transiently shaped using a specific microfluidic channel geometry, followed by polymerization of the AESO component and subsequent removal of the silicon oil through solvent dissolution. The resultant particle consists solely of pAESO, imprinted by the process. **Figures 3A** and **3B** depict the configurations employed: (i) in the first example, a Y-shape mixer is introduced upstream of the flow focusing device to generate silicon oil/AESO Janus droplets; (ii) in the second example, a double flow focusing structure is utilized to create silicon oil in AESO in water droplets. Polymerization occurs exclusively in the AESO phase due to the presence of the photo-initiator when the droplets are transported through the UV exposure region of the chip. After collection, unpolymerized silicone oil is removed by acetone rinsing.

Depending on the experimental configuration, crescent-moon-shaped or hollow pAESO particles with excellent regularity in shape and size can be obtained.

Fabrication of AESO capsules using microfluidics

We create capsules by utilizing AESO as a shell that encapsulates an aqueous core. To achieve this, we modify the initial microfluidics chip design by incorporating a third outlet, resulting in two flow focusing junctions. The underlying principle remains consistent throughout the emulsion process, maintaining equilibrium between the pressures exerted by the three phases. The channels of the chips are segmented to facilitate the shearing of the inner phase by an oil phase at the first junction, which is then subsequently sheared by the continuous aqueous phase. This necessitates two distinct wettability behaviors: lipophilic up to the first junction and hydrophilic thereafter. To achieve this, we selectively functionalize the second junction only with PVP [25]. The first part is subjected to compressed air injection to prevent the hydrophilic treatment from permeating through.

In terms of formulations, we introduce 2 wt.% of Span 80 [26] as a surfactant to the oil phase for emulsification between the core and the shell. The final concentration of AESO is adjusted to 40 wt% in a 1-octanol solvent to ensure proper shearing. Additionally, we incorporate 1 wt% of the photo-initiator Irgacure 819 in an acetone solution. The inner phase is prepared with 0.12 mg/mL Dextran marked by the fluorophore Alexa Fluor 647. The new continuous phase is composed of 15 wt% Pluronic F-68 as a surfactant for the second emulsion, along with 10 wt% Tween-20 as a viscosifier for the aqueous phase.

Utilizing a dripping regime for the initial junction and a jetting regime for the second, we achieve an alternating fabrication process between capsules and straightforward AESO droplets. Following this, the entire set undergoes an initial photopolymerization at 365 nm within the chip's serpentine, after which they are dispersed and rinsed in acetone. Subsequently, a second UV exposure takes place using a 0.4 vol.% solution of Irgacure 819 for photopolymerization, followed by another rinsing phase.

For the analysis of the capsules, we leverage the fluorescent properties of each phase constituting the capsules. Notably, fluorescent spectrometry analysis reveals an autofluorescence of the AESO reagent, which diminishes when incorporated into the oil phase of the outer shell. Consequently, the solution emits light when excited at 425 nm. In contrast, the inner phase is marked by a fluorophore at 630 nm, where the oil phase's sensitivity is nearly negligible, especially when compared to the core, as shown in **Fig. S6**.

Loading capacity of AESO particles for organic fluorescent molecules

Polymeric microparticles are frequently rendered fluorescent and employed as probes in hydrodynamic experiments [27], biochemical assays [28], and biological studies [29]. In consideration of these diverse applications, we have devised two strategies to load amphiphilic and hydrophobic fluorescent molecules, creating a versatile platform for various applications.

The first method involves a straightforward soaking experiment, where a specific quantity of pAESO particles is immersed in an acetone solution of a lipophilic dye, Nile Red [30], as described in **Figure 4A**, for varying durations (10 min, 24 h, and 72 h). The fluorescence of these particles is then examined using a confocal microscope to assess the diffusion effect.

As illustrated in **Figure 4B**, the fluorescence of Nile Red is observed within the particles for all three samples. Specifically, fluorescence is initially found only around the edge of the particles after a 10-minute soaking, but nearly the entire cross-section of the particles exhibits fluorescence after 72 hours of soaking. **Figure 4C** presents the normalized line profiles of fluorescence intensity along the diameter of pAESO particles for these three samples, clearly illustrating the gradient of fluorescence from the edge to the center of the particles. This observation suggests that samples with longer soaking times possess greater diffusion depth and intensity of fluorescence within the particles.

In the second approach, we combine headgroup-modified fluorescent phospholipids (DOPE-CF) with AESO as the dispersed phase at a concentration of 0.1 mg/mL as described in **Figure 4D**. The resulting fluorescent particles are fabricated using the

microfluidic device mentioned above. The synthesized pAESO particles exhibit homogeneous green fluorescence, as depicted in **Figure 4E** and **4F**, and this fluorescence is maintained throughout the UV exposure preparation process.

Chemical and enzymatic degradation of AESO particles

To investigate the degradation property of synthesized pAESO microparticles, we incubate a certain amount of pAESO particles in the different conditions and periodically monitor their morphology changes and mass loss for a long term. The following conditions are performed in the degradation experiments: (i) 3 wt.% KOH aqueous solution at room temperature (R.T.), (ii) 3 wt.% KOH alcoholic solution at R.T., (iii) 3 wt.% KOH alcoholic solution at 70 °C, (iv) 150 units/mL esterase aqueous solution at R.T., (v) 700 units/mL lipase aqueous solution at R.T. The pAESO particles display the highest degradation rate in the hot alkaline alcoholic solution, as shown in **Figure 5A**. The suspension of pAESO particles becomes transparent and particles are completely hydrolyzed so that we observe nothing under the microscope after 1 h incubation. While it will take 19 hours to complete the hydrolysis with the condition (ii). On the contrary, even after ca. 250 hours of incubation with the condition (iii), there are still a small amount of particle fragments remaining in the vial.

Figure 5C shows the enzymatic degradation curve under the action of esterase and lipase. pAESO particles present good enzymatic degradability under both conditions in a short time. The particles exhibit a faster rate of hydrolysis in the lipase in the early stage. Following the time lapsing, the hydrolysis rates of the particles under each condition gradually slow down and reach a plateau after 6 days, at which time about 35% of the particles were degraded. In order to study the actions of different enzymes on the degradation of pAESO particles, we measure the surface roughness of the enzyme treated particles, as shown in **Figure 5D**. Compared to the original particles, the roughness of the particles greatly increased from 3.07 nm to 14.4 nm after incubation with esterase for 14 days, as depicted in **Figure 5E**. On the contrary, the roughness of lipase treated particles has only a slight increase, which is basically maintained at the same level as the original particles.

DISCUSSION

Optimization and evaluation of AESO particles preparation

We present two accessible methods for fabricating AESO particles through emulsion polymerization, with emulsification being a crucial step in the process. The formation of droplets involves a competition between interfacial force and viscous force [31], and the inherently high viscosity of AESO (~18000-32000 mPa·s) tends to impede this process. To overcome this challenge, we incorporate a solvent, 1-octanol, to reduce the viscosity of AESO. Additionally, since 1-octanol exhibits suitable solubility (0.3 g/L) in water, it does not hinder the emulsification process and can be easily removed by diffusion into the water phase post-polymerization.

Qualitative analysis based on FTIR microscope results suggests that a higher initiator concentration promotes the polymerization of AESO droplets. However, prolonged exposure time does not contribute to increase monomer conversion significantly. We posit that a system with a high initiator concentration (exceeding 0.4 wt.%) becomes overly sensitive to light, where even ambient light may trigger reactions, leading to challenging manipulation. Therefore, we propose that a 0.4% (m/v) initiator concentration and a 2-minute UV exposure represent appropriate conditions for synthesizing polydisperse particles.

Morphology analysis of AESO particles

The static precursor droplets maintain a spherical shape due to surface tension, resulting in synthesized particles with the same shape during reticulation (see **Figure 1B, C**). However, in the case of dynamically generated and cross-linked droplets through microchannels, heart-shaped AESO particles are obtained instead of the usual round ones (see **Figure 2C**). Similar heart-shaped particles of poly(ethylene glycol) diacrylate (PEG-DA) were also prepared and observed by Cai et al. [32]. A commonly accepted explanation is that the droplets flow along the center of the channel, where the velocity is faster than in the continuous phase near the channel wall. This velocity gradient in the

direction perpendicular to the flow generates a shear stress opposite to the flow direction on the droplets. It is certain that the net flux of the circulation originating from the shear stress is zero inside the droplets, and the pressure at the front of the droplets is larger than at the lagging edge. Consequently, a backward flow occurs near the interface, while a forward compensation flow takes place in the center of the droplet. As a result, the heart-shaped droplets form, following an increase in the curvature of the leading edge and a decrease in the curvature of the trailing edge, which can be maintained through the reticulation process.

Dispersion behavior of AESO particles in different solvents

The AESO particles extracted from the microfluidic chip exhibit distinct dispersion behaviors in both aqueous and organic environments, as illustrated in **Figure 2E**. We attribute this variance to the incomplete polymerization of AESO particles, stemming from two possible factors. Firstly, the initiation of AESO droplets solely occurs in the serpentine region of the microfluidic chip under UV light. However, the high flow velocity results in a brief retention time (less than 1 s) for irradiation. Concurrently, dissolved oxygen in the reactants may capture and consume free radicals, forming inactive peroxy radicals that inhibit monomer polymerization [33] . The high oxygen permeability of the PDMS channel further supplements oxygen from the surroundings [34]. The combination of these factors severely impedes the curing of AESO particles at the oil-water interface, leading to the aggregation of particles with a sticky hydrophobic surface. The presence of gelatinous substances around the particles, as depicted in **Figure 2F**, suggests incomplete polymerization of AESO. This observation aligns with findings in a previous study by K. Krutkramelis et al. [35], focusing on a water-in-oil (w/o) system of PEG-DA in a microfluidic device.

Upon re-exposing these particles with 0.4% (w/v) initiator under UV light for 2 minutes in acetone, they demonstrate improved dispersibility in an aqueous buffer of PB-Tween 20. Additionally, examination of the SEM images (**Figure 2F**) reveals the disappearance of the sticky gel, indicating that the particles no longer trap each other upon contact. These

results substantiate our earlier assumption. This method can also serve as a post-treatment approach to produce fully polymerized AESO particles following the microfluidic route.

Fluorescent rendering of the pAESO particles

We detailed two simple ways (premixing and diffusion) to load AESO particles with two different organic molecules for fluorescent functionalization. Both products present a homogeneous fluorescence in the whole cross section. Lee et al. [36] also report the incorporation of dye into PS microspheres with a similar swelling-diffusion method. However, in their work the dyes prefer to form a separate phase within the matrix, giving rise to the heterogeneous fluorescence. The different phenomenon from two kinds of materials may be due to the different monomer molecular structures. The long branches derived from fatty acids in AESO molecules, as shown in **Figure S1A**, may cause the steric hindrance to restrict the molecule conformation, and result in a looser network, which provides larger free volume for swelling and diffusion of small fluorescent molecules from external sources. In addition, the good compatibility between AESO and dye molecules is the other crucial reason. These properties of AESO particles may be developed to load and encapsulate other functional organic molecules for extensive applications, such as drug carriers.

Degradation of AESO particles

AESO particles contain abundant ester bonds derived from triglycerides and acrylate groups, offering the potential for hydrolysis of polymerized AESO. Our results demonstrate that AESO particles exhibit good degradability in both chemical and enzymatic environments, particularly in hot alkaline organic solutions. We hypothesize that a small portion of KOH converts into a stronger alkaline potassium ethoxide in hot ethanol [37]. Additionally, the swelling of AESO in organic solvents (refer to **Figure 5A**) and high temperatures facilitate molecular diffusion, making it easier for alkaline molecules to permeate the particles. This leads to a larger interface, enhancing hydrolysis. In contrast, water, as a poor solvent for AESO, may disrupt the action of the

water phase on the particle surface, reducing the hydrolysis rate. The degradation of hydrophobic AESO particles in an aqueous solution will require more time.

In enzymatic degradation experiments, both esterase and lipase can be employed for the hydrolysis of esters. While esterase prefers attacking the ester bonds in short-chain fatty acids (the acrylate in AESO), lipase tends to break the ester bonds in triglycerides [38,39] (see **Figure 5B**). Clearly, compared to the acrylate acting as the cross-linking group of AESO, the extensively present glyceride is easier to hydrolyze, potentially explaining the higher degradation rate observed with lipase. Furthermore, the difference in molecular size between lipase (molecular weight approximately 50 kDa) [40] and esterase (molecular weight approximately 148 kDa) is another crucial factor influencing their behaviors in the early stage. This difference is evident in their impact on particle surface roughness during the degradation process, as depicted in **Figure 5D and E**. Nevertheless, the enzymes gradually become inactivated over the long term, leading to both samples reaching a degradation plateau.

Overall, in comparison to traditional polymers like PE [41] and PET [42], the degradation of AESO can be achieved in a milder and more flexible manner, without costly reaction medium, harsh conditions or specific equipment, which may serve as a promising recyclable and degradable material.

Release of a model drug, ibuprofen, in biomimic environments

Ibuprofen is a non-steroidal drug, which can inhibit cyclooxygenase and reduce the generation of prostaglandins, resulting in analgesic and anti-inflammatory effects. It is thus widely used for the treatment of pain, fever, and inflammation [43]. However, the structure of arylalkanoic acid (see **Figure 6A**) gives rise to a short serum half-life of 1.8 to 2 hours. Patients have to suffer the frequent administration of 3 or 4 times per day, which usually leads to side effects, such as gastrointestinal toxicity, ulcer, etc [44]. In addition, the bioavailability of ibuprofen is low due to its poor solubility in water, making the use of microcarriers to encapsulate and release ibuprofen an interesting solution to get over these disadvantages. Here, we mix 15 mg ibuprofen with a photosensitive AESO solution (65 % (m/m) AESO/1-octanol and 0.4 % (v/v) Irgacure 819). This oil

solution is emulsified and polymerized to prepare the ibuprofen loaded AESO (Ibu-pAESO) particles. We obtain the synthesized Ibu-pAESO particles with a diameter of 20.5 ± 8.3 μm, whose morphology remains the same as the original particle, as shown in **Figure 6B**.

We carry out the *in vitro* release assay of ibuprofen by incubating 50 mg of Ibu-pAESO particles in two model environments: a simulated intestinal fluid (SIF, pH=6.8) and a simulated gastric fluid (SGF, pH=1.3), which are used to mimic the release media during the oral administration. The UV-Vis absorption at 220 nm of the supernatant is monitored at given time intervals to characterize the drug released from the particles into the aqueous phase. The cumulative ibuprofen release curve is displayed in **Figure 6C**, demonstrating the similar trends of ibuprofen release in the media with different pH values. After the incubation in SGF for 4 h, 43 % of ibuprofen releases from the Ibu-AESO particles, and the cumulative release ratio increases up to 73 % by 144 h. On the other hand, the ibuprofen release is more rapid in the SIF, where the release ratio is 58 % in the first 4 h and reaches 83 % after 144 h. Ibuprofen release seems not due to Ibu-pAESO esters hydrolysis in acidic conditions, since less ibuprofen is released in more acidic medium. This distinguishing behavior can be likely attributed to the pH-dependence of the solubility of ibuprofen in water, which is in agreement with the previous reports [45,46]. The experimental dissolution data are well described by a Korsmeyer–Peppas model in both model fluids (see **Figure S5 and Table S1** for details, equations and fits), with parameters compatible with an ibuprofen release governed by a quasi-Fickian diffusion mechanism, consequence of the concentration gradient with the liquid phase. In addition, we can calculate the mean dissolution time (MDT) of ibuprofen in SGF and SIF conditions, which are equal to 4.1 h and 6.9 h respectively, which indicates the efficiency of the AESO microparticles to delay the release of the drugs.

CONCLUSION

In summary, we propose employing two straightforward emulsification photo-polymerization methods to create AESO particles using a vortex mixer and a

microfluidic device. Our research demonstrates that the size and shape of these particles can be easily customized by precisely adjusting the hydrodynamics of the flow and modifying the microfluidic chip design. The synthesized AESO particles exhibit excellent optical properties within the mid-infrared range and the ability to accommodate amphiphilic or hydrophobic fluorescent molecules for functionalization. Furthermore, they can serve as soft shells to encapsulate other substances. Leveraging the numerous ester bonds present in the thermoset, AESO particles exhibit notable degradability under both chemical and enzymatic conditions. This characteristic positions them as potential candidates for the development of recyclable, degradable, and functional materials. Additionally, their ability to encapsulate and release functional substances of the medical field could open avenues for innovative and eco-friendly pharmaceutical products. These developments align with the industry's growing emphasis on sustainability and could pave the way for compliant and environmentally responsible microparticulate products.

AUTHORS CONTRIBUTIONS

CH, EL and JF designed the experiments, CH, EL and LL performed the experiments, ND and CH performed the FT-IR microscopy experiments. BB, CH and EL performed the SEM and AFM data collection and analysis. JMM participated in the drug release experimental design and data analysis. JF designed and supervised the study. All authors participated in the analysis of the data, CH, EL and JF wrote the manuscript.

FUNDING

This work has received support of “Institut Pierre-Gilles de Gennes” (Laboratoire d’excellence: ANR-10-LABX-0031 PSL, “Investissements d’avenir”: ANR-10-IDEX-0001-02 PSL and Equipement d’excellence: ANR-10-EQPX-0034 PSL). C.H. and J.F. gratefully acknowledges the financial support of CSC (China Scholarship Council) and CentraleSupélec.

AVAILABILITY OF DATA

The data of this study are available upon request.

ACKNOWLEDGEMENTS

The authors gratefully acknowledge Kevin Phan (Institut Pierre-Gilles de Gennes), Dr. Bertrand Cinquin (Institut Pierre-Gilles de Gennes) and Dr. Thomas Le Saux (Chemistry Department, ENS, Paris) for their respective help on the microfabrication, confocal microscopy and fluorescence analysis.

REFERENCES

[1] M. Okada, *Prog. Polym. Sci.* **2002**, *27*, 87.
[2] T. Saito, T. Uematsu, S. Kimura, T. Enomae, A. Isogai, *Soft Matter* **2011**, *7*, 8804.
[3] L. A. M. van den Broek, R. J. I. Knoop, F. H. J. Kappen, C. G. Boeriu, *Carbohydr. Polym.* **2015**, *116*, 237.
[4] H. Nabipour, X. Wang, L. Song, Y. Hu, *Carbohydr. Polym.* **2020**, *246*, 116641.
[5] A. Tribot, G. Amer, M. Abdou Alio, H. de Baynast, C. Delattre, A. Pons, J.-D. Mathias, J.-M. Callois, C. Vial, P. Michaud, C.-G. Dussap, *Eur. Polym. J.* **2019**, *112*, 228.
[6] N. B. Samarth, P. A. Mahanwar, *OJOPM* **2015**, *05*, 1.
[7] Y. Xia, R. C. Larock, *Green Chem.* **2010**, *12*, 1893.
[8] B. Cakmakli, B. Hazer, I. O. Tekin, F. B. Cömert, *Biomacromolecules* **2005**, *6*, 1750.
[9] R. C. Larock, X. Dong, S. Chung, Ch. K. Reddy, L. E. Ehlers, *J. Am. Oil Chem. Soc.* **2001**, *78*, 447.
[10] F. C. Naughton, *J. Am. Oil Chem. Soc.* **1974**, *51*, 65.
[11] N. Spiccia, E. Border, J. Illesinghe, W. Jackson, A. Robinson, *Synthesis (Mass)* **2013**, *45*, 1683.
[12] R. Slivniak, A. Ezra, A. J. Domb, *Pharm. Res.* **2006**, *23*, 1306.
[13] D. Behera, A. K. Banthia, *J. Appl. Polym. Sci.* **2008**, *109*, 2583.
[14] H.-M. Kim, H.-R. Kim, B. S. Kim, *J. Polym. Environ.* **2010**, *18*, 291.
[15] H. Pelletier, N. Belgacem, A. Gandini, *J. Appl. Polym. Sci.* **2006**, *99*, 3218.
[16] Z. Liu, B. H. Tisserat, *Industrial Crops and Products* **2018**, *112*, 196.

[17] M. Fernandes, A. P. Souto, M. Gama, F. Dourado, *Nanomaterials (Basel)* **2019**, *9*.
[18] S. Miao, W. Zhu, N. J. Castro, M. Nowicki, X. Zhou, H. Cui, J. P. Fisher, L. G. Zhang, *Sci. Rep.* **2016**, *6*, 27226.
[19] E. Baştürk, M. V. Kahraman, *J. Appl. Polym. Sci.* **2016**, *133*.
[20] L. R. de Souza, B. Whitfield, A. Al-Tabbaa, *Sustainability* **2022**, *14*, 13556.
[21] R. Tajau, M. I. Ibrahim, N. M. Yunus, M. H. Mahmood, M. Z. Salleh, N. G. N. Salleh, AIP Conference Proceedings; AIP Publishing LLC, 2014; pp. 164–169.
[22] B. L. Mojet, S. D. Ebbesen, L. Lefferts, *Chem. Soc. Rev.* **2010**, *39*, 4643.
[23] C. B. Provis-Evans, E. H. E. Farrar, M. N. Grayson, R. L. Webster, A. K. Hill, *Anal. Chem.* **2020**, *92*, 7500.
[24] M. Barde, K. Avery, C. W. Edmunds, N. Labbé, M. L. Auad, *ACS Sustain. Chem. Eng.* **2019**, *7*, 2216.
[25] S. Hemmilä, J. V. Cauich-Rodríguez, J. Kreutzer, P. Kallio, *Appl. Surf. Sci.* **2012**, *258*, 9864.
[26] R. Dreyfus, P. Tabeling, H. Willaime, *Phys. Rev. Lett.* **2003**, *90*, 144505.
[27] M. Frankowski, J. Theisen, A. Kummrow, P. Simon, H. Ragusch, N. Bock, M. Schmidt, J. Neukammer, *Sensors* **2013**, *13*, 4674.
[28] C. van der Wel, G. L. van de Stolpe, R. W. Verweij, D. J. Kraft, *J. Phys. Condens. Matter* **2018**, *30*, 094005.
[29] F. Del Giudice, M. Tassieri, C. Oelschlaeger, A. Q. Shen, *Macromolecules* **2017**, *50*, 2951.
[30] P. Greenspan, E. P. Mayer, S. D. Fowler, *J. Cell Biol.* **1985**, *100*, 965.
[31] E. Roumpea, N. M. Kovalchuk, M. Chinaud, E. Nowak, M. J. H. Simmons, P. Angeli, *Chem. Eng. Sci.* **2018**, *195*, 507.
[32] Q.-W. Cai, X.-J. Ju, C. Chen, Y. Faraj, Z.-H. Jia, J.-Q. Hu, R. Xie, W. Wang, Z. Liu, L.-Y. Chu, *Chemical Engineering Journal* **2019**, *370*, 925.
[33] L. B. Levy, *Plant/Oper. Prog.* **1987**, *6*, 188.
[34] C. Bouquerel, W. César, L. Barthod, S. Arrak, A. Battistella, G. Gropplero, F. Mechta-Grigoriou, G. Zalcman, M. C. Parrini, M. Verhulsel, S. Descroix, *Lab Chip* **2022**, *22*, 4443.
[35] K. Krutkramelis, B. Xia, J. Oakey, *Lab Chip* **2016**, *16*, 1457.
[36] J.-H. Lee, I. J. Gomez, V. B. Sitterle, J. C. Meredith, *J. Colloid Interface Sci.* **2011**, *363*, 137.
[37] K. Chandran, R. Nithya, K. Sankaran, A. Gopalan, V. Ganesan, *Bull. Mater. Sci.* **2006**, *29*, 173.
[38] P. Fojan, P. H. Jonson, M. T. Petersen, S. B. Petersen, *Biochimie* **2000**, *82*, 1033.
[39] H. Chahinian, L. Sarda, *Protein Pept. Lett.* **2009**, *16*, 1149.
[40] R. Verger, G. H. De Haas, L. Sarda, P. Desnuelle, *Biochimica et Biophysica Acta (BBA) - Protein Structure* **1969**, *188*, 272.
[41] H.-M. Feng, J.-C. Zheng, N.-Y. Lei, L. Yu, K. H.-K. Kong, H.-Q. Yu, T.-C. Lau, M.

H. W. Lam, *Environ. Sci. Technol.* **2011**, *45*, 744.
[42] J. R. Campanelli, M. R. Kamal, D. G. Cooper, *J. Appl. Polym. Sci.* **1993**, *48*, 443.
[43] W. T. Beaver, *Int. J. Clin. Pract. Suppl.* **2003**, 13.
[44] S. A. Furey, J. A. Waksman, B. H. Dash, *Pharmacotherapy* **1992**, *12*, 403.
[45] K. A. Levis, M. E. Lane, O. I. Corrigan, *Int. J. Pharm.* **2003**, *253*, 49.
[46] L. R. Shaw, W. J. Irwin, T. J. Grattan, B. R. Conway, *Drug Dev. Ind. Pharm.* **2005**, *31*, 515.

FIGURES

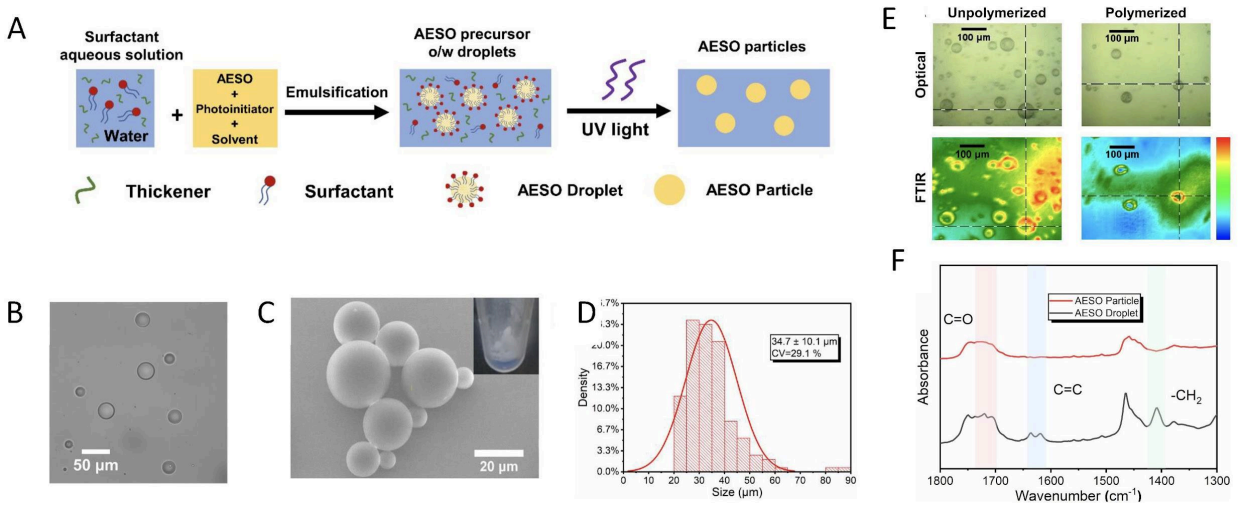

Figure 1. A) Schematic of AESO microparticle fabrication routine via oil emulsification and photopolymerization. B) Optical microscope image of AESO droplets. C) SEM image of AESO particles. D) Size distribution plot of AESO particles fitted with the normal distribution (average diameter = 34,7 $\pm$ 10,1 μm, CV = 29.1%). E) Optical images and their corresponding infrared absorbance plot of spectral slices under 1635 cm^{-1} of AESO droplets before and after polymerization, which were taken through FTIR microscope. F) FTIR spectra of the points indicated by the dashed cross in FTIR images.

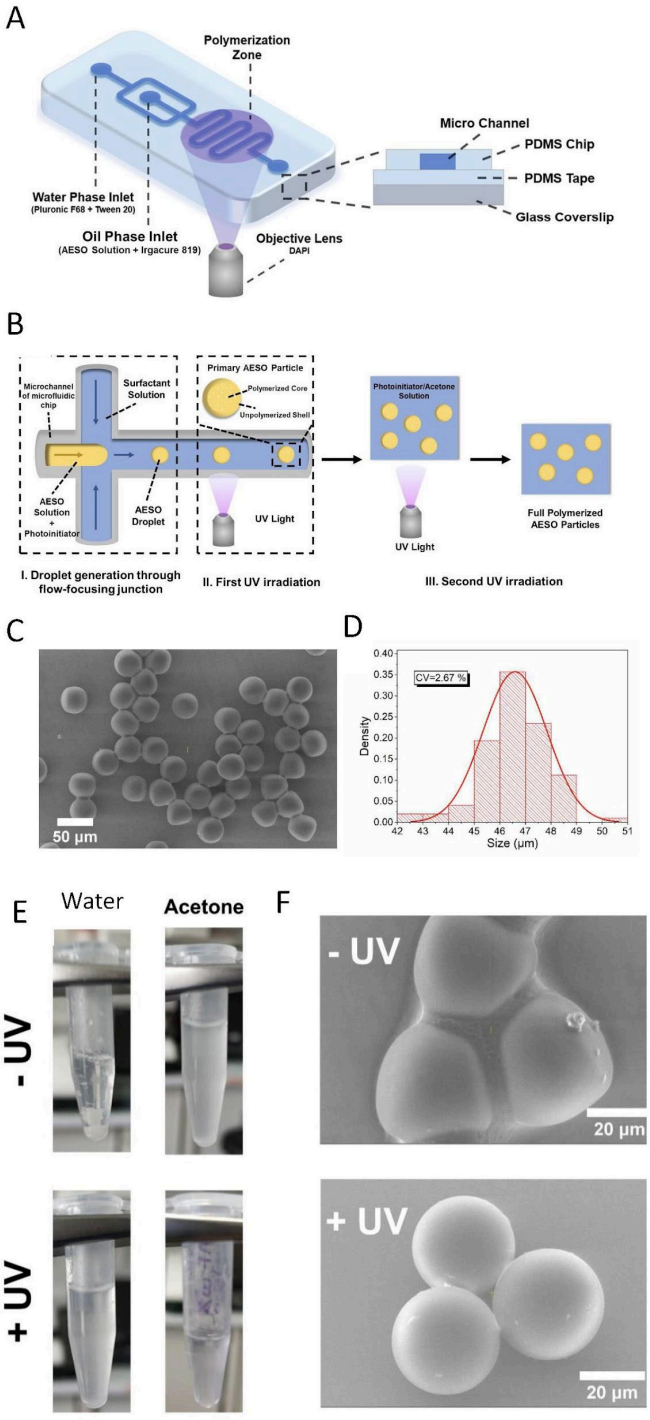

Figure 2. A) Schematic of a “one pot” microfluidic chip for preparation of monodispersed AESO microparticles. B) Partially enlarged schematic side view shows the multilayer structure of the chip, in which a PDMS coated glass slide is used as the substrate. C) SEM image of AESO particles prepared by microfluidic chip. D) Size distribution plot of

AESO particles fitted with the normal distribution (average diameter = 46,6 ± 1.24 µm, CV = 2.67%). E) Dispersed states of the particles in water and acetone. F) Corresponding SEM images of AESO particles out of chip and AESO particles with secondary UV exposure.

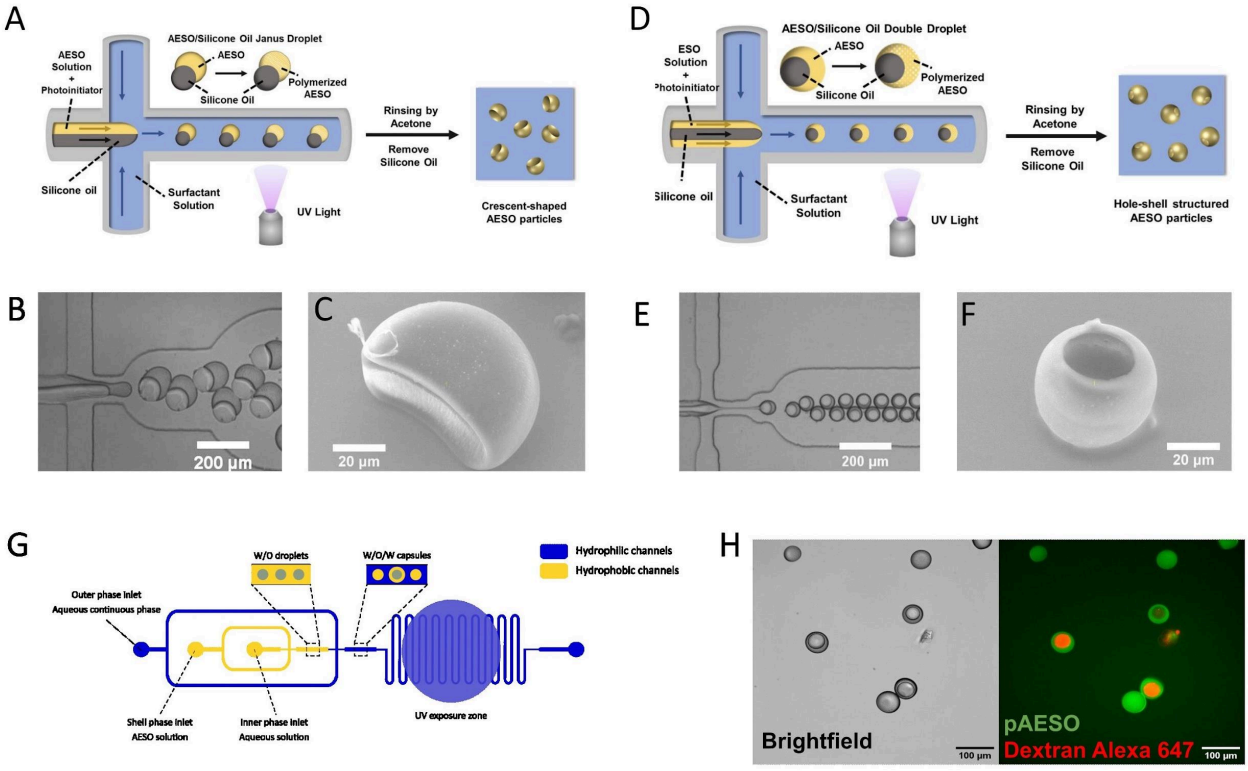

Figure 3. Fabrication schematic, optical microscopy images of precursor droplets and SEM images of the crescent-moon-shaped (A,B and C respectively) and hollow-structured pAESO particles (D, E and F respectively). G) Schematic of microfluidic chip for pAESO microcapsules. H) Optical and fluorescent images of the AESO microcapsules containing a core solution of dextran Alexa 647. Exc. wavelengths = 488 and 630nm.

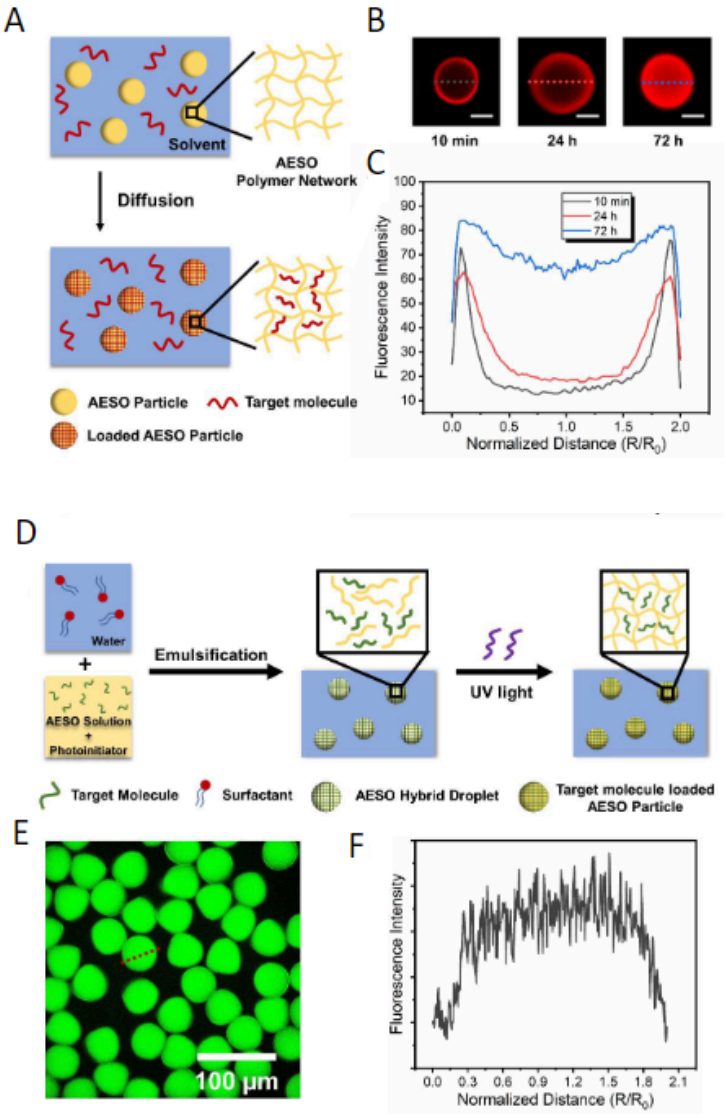

Figure 4. (A) Schematic of the loading target molecules on pAESO particles by diffusion method. (B) Fluorescent images by confocal microscopy of the pAESO particles after soaking in Nile red acetone solution for 10 min, 24 h, 72 h. Exc. Wavelength = 488 nm, scale bar = 15 μm. (C) Fluorescence line profiles of the AESO particles along the dotted lines shown in (B). (D) Schematic of the loading target molecules on AESO particles by pre-mixing method. (E) Fluorescence image of the AESO particles containing 0.1 mg/mL lipid DOPE-CF. Exc. wavelength = 488 nm. (F) Fluorescence line profile of the AESO particles along the dotted line shown in (E).

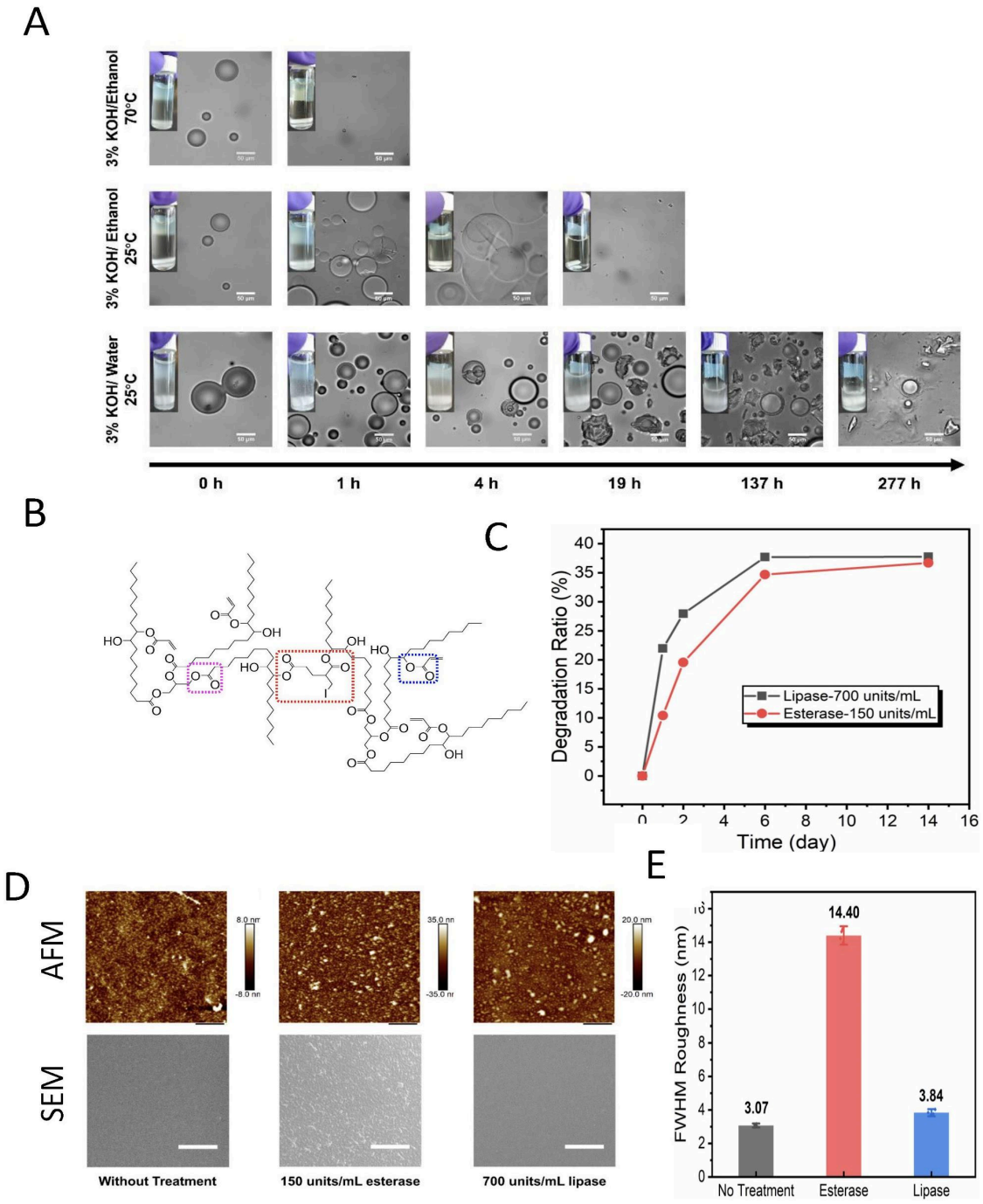

Figure 5. A) Microscopic and macroscopic (inset) appearances of the AESO particles with aqueous and ethanol solution of 3 wt.% KOH at room temperature and at 70 °C after 0, 1, 4, 19, 137, 277 h. B) Schematic of an AESO dimer, where "-I" represents the residue of the initiator. The red box indicates the position where the polymerization

occurs. The pink and blue boxes indicate the ester bonds in two different chemical environments in the AESO molecule. C) Enzymatic degradation curves of the AESO particles by esterase and lipase, with the weight loss as a function of time. D) AFM images of the AESO particles surface without treatment, treated by esterase and lipase for 14 days, the SEM images showed the surface morphology of each sample. Scale bar = 1 μm. E) Full width half maximum roughness of pAESO particles, comparing degradation by esterase or lipase enzymes.

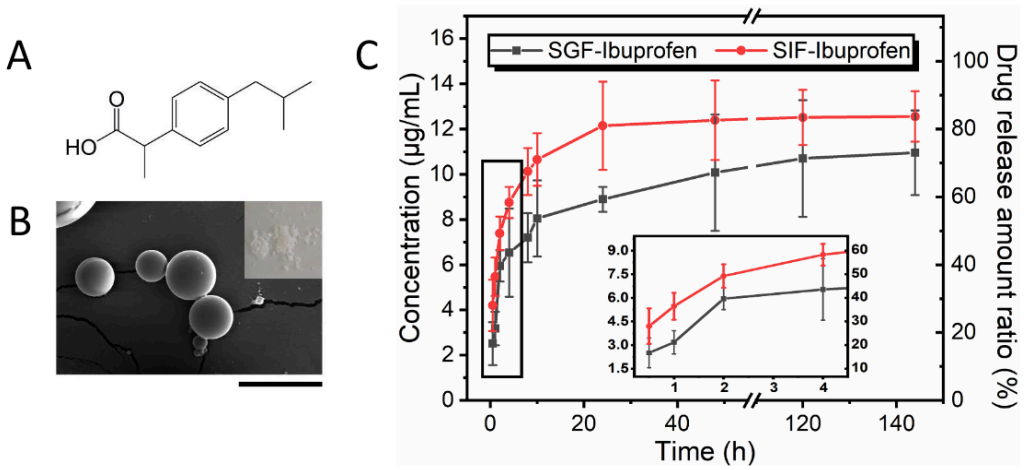

Figure 6. (A) Structure of the ibuprofen molecule (B) SEM image of the ibuprofen loaded pAESO particles. The inset photo shows the corresponding powder. (C) Release curves of ibuprofen from AESO particles in SGF and IGF simulated body fluid (inset : enlarged view of the initial part of the curves).

TOC/Abstract Graphic.

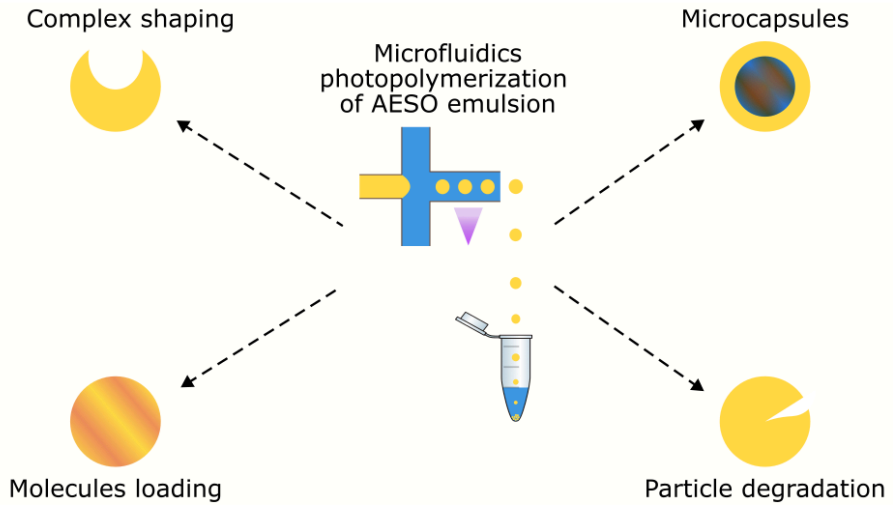

Caption : Acrylated epoxidized soybean oil is used as a biosourced material to fabricate sophisticated, functional and degradable microparticles using microfluidics